MODELLING THE TRANSIENT ANALYSIS OF FLAT MINIATURE HEAT PIPES IN PRINTED CIRCUIT BOARDS USING A CONTROL VOLUME APPROACH

W.W. Wits and J.B.W. Kok
University of Twente, Faculty of Engineering Technology, Enschede, The Netherlands

Abstract

The heat pipe is a two-phase cooling solution, offering very high thermal coefficients, for heat transport. Therefore, it is increasingly used in the design of electronic products. Flat miniature heat pipes are able to effectively remove heat from several hot spots on a Printed Circuit Board (PCB). A model based on control volume elements is presented in this paper to analyze the behaviour of flat miniature heat pipes. The advantage of this approach, compared to finite element models, is that the model can be expanded with additional evaporator or condenser components very easily. Actual PCBs with multiple hot spots, cooled by flat miniature heat pipes, and the parameter effects can be analyzed very quickly, without the necessity of complex and time-consuming finite element analysis.

Nomenclature

A	area [m^2]	m	mass [kg]	**Subscripts**	
γ	inclination angle [rad]	$\dot{m}$	mass flux [kg/s]	c	condenser
c	specific heat [J/kg·K]	P	pressure [Pa]	e	evaporator
D	diameter [m]	Q	heat, power [W]	eff	effective
fRe	Reynolds friction factor	ρ	density [kg/m^3]	eq	equivalent
g	acceleration of gravity [m/s^2]	R	thermal resistance [K/W]	h	hydraulic
h	liquid height [m]	r	radius [m]	l	liquid
h_{fg}	latent heat [J/kg]	σ	surface tension [N/m]	ss	steady state
k	thermal conductivity [W/m·K]	T	temperature [K]	v	vapour
l	length [m]	V	volume [m^3]		
μ	dynamic viscosity [kg/m·s]	v	velocity [m/s]		

1 Introduction

The on-going process of miniaturization and hence increasing thermal power density of electronic components, forces engineers to develop new cooling solutions. Techniques based on single phase convection or solid conduction, lack sufficient cooling capacity on small components. Therefore two-phase cooling solutions (e.g. heat pipes), offering higher thermal coefficients, are increasingly used in the design of electronic products.

A heat pipe is composed of four essential parts: an evaporator (1), where heat is consumed by vaporization, a vapour transport section (2) transporting the hot vapour to a condenser, a condenser (3) that extracts the heat and condenses the vapour, and a liquid transport section (4) that returns the condensate to the evaporator. This way, the evaporator can transport heat, at very low temperature gradients, from a hot spot to a cold spot, where the condenser is located.

In a previous publication of this study (Wits et al., 2006) a new heat pipe design was presented. A heat pipe was fully integrated into a PCB, using only established PCB production and surface mount assembly techniques. The manufactured prototype is shown in Figure 1(a). A typical multilayer PCB consists of polymeric layers pressed together with bonding layers in between. On each polymeric layer a metallic pattern can be produced. This feature is utilized to fabricate a wick structure to transport the condensate from the hot spot to the cold spot inside the PCB. The heat pipe vapour space is realized by machining a cavity in an intermediate layer. Figure 1(b) illustrates an embedded heat pipe using one (thicker) intermediate layer. The height of the heat pipe can also be varied by stacking multiple layers in between the heat pipe's top and bottom layer. As the polymeric laminates and bonding layers are permeable to both water and gases, a copper plated groove is fabricated around the heat pipe cavity, ensuring a hermetically sealed enclosure.

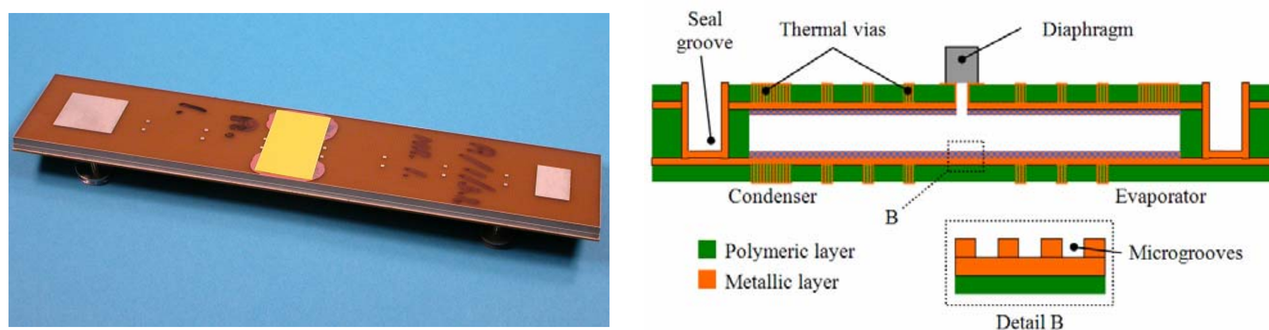

(a) manufactured prototype *(b) schematic layout*

Figure 1: *Heat pipe integrated in a printed circuit board.*

The wick structure of the heat pipe, shown in Detail B, is composed of axially oriented capillary microgrooves, realized by a selective plating process. Groove dimensions can be optimized to the applicable production process. Experiments indicated a minimum groove width of 50μm, based on conventional dry film lithography. Below this boundary, the resist stripping process used showed problems to effectively strip the resist from the microgrooves after plating.

In the evaporator and condenser region, the heat must travel through the laminated PCB layers. These polymeric layers are poor thermal conductors; hence to transfer the heat into and out of the embedded heat pipe, an array of thermal vias is placed at both the evaporator and condenser locations.

After depressurization, the empty heat pipe cavity is filled with water (deoxidized and decontaminated) by inserting a scaled needle through the diaphragm. The heat pipe should be charged with just enough water to fill the microgrooves.

2 Control volume model

During operation, a heat pipe can encounter various limitations. In the application of electronics cooling the most critical limitation for flat miniature heat pipes is the capillary limit (Cao et al., 1993). This limit is reached when the wick structure cannot pump sufficient working fluid to the evaporator region. To analyze this transient effect, the heat pipe is divided into control volume elements (Vincent and Kok, 1992). In the case of a single evaporator heat pipe, there are four elements: an evaporator and a condenser region, and a liquid and vapour transport section, as illustrated in Figure 2(a). As control volume elements are used, the model can be expanded with additional evaporator or condenser components very easily. For instance, a model expansion for one additional evaporator is shown in Figure 2(b).

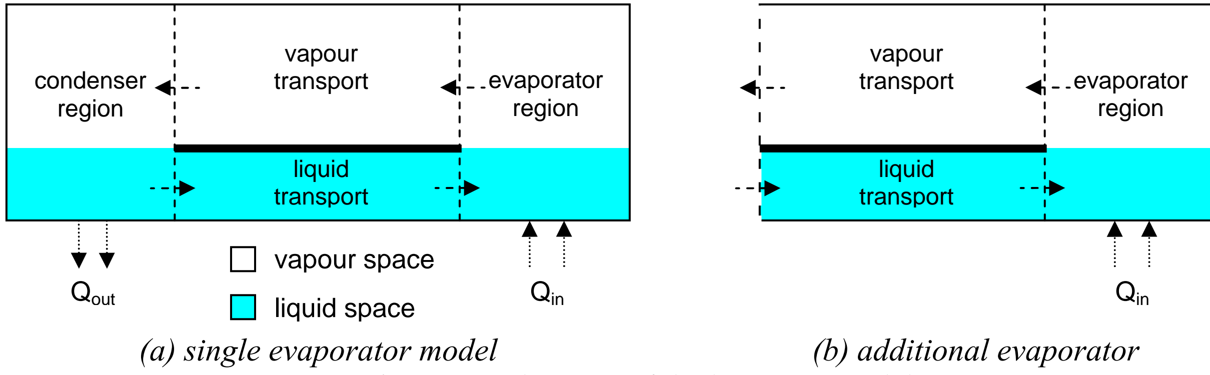

(a) single evaporator model *(b) additional evaporator*

Figure 2: *Schematic of the heat pipe model.*

Assuming an adiabatic vapour and liquid transport, the continuity equation of an evaporator or condenser region simplifies to a balance of mass fluxes, as illustrated in Figure 3. This balance is formulated as:

$$\frac{d}{dt}[m] = \dot{m}_{l,in} - \dot{m}_{l,out} + \dot{m}_{v.in} - \dot{m}_{v,out} \quad \Rightarrow \tag{1}$$

$$A\frac{d}{dt}[h\rho_l] = A_l(\rho_{l,in}v_{l,in} - \rho_l v_{l,out}) + A_v(\rho_{v,in}v_{v,in} - \rho_v v_{v,out}) \tag{2}$$

As the heat pipe is hermetically sealed, a condenser or evaporator region located at the end of the heat pipe cannot have any in and out flow of mass from the sealed side. Therefore at the heat pipe ends, the two corresponding terms in Equation (1) become zero. In the steady state all continuity equations will cancel each other out, as the vapour and liquid mass flow will be equal. However, in a transient situation energy storage is made possible by a fluctuating liquid height (*h*) in the grooves. The vapour is assumed to be in a saturated state throughout this analysis. This couples vapour pressure and vapour temperature directly to one other.

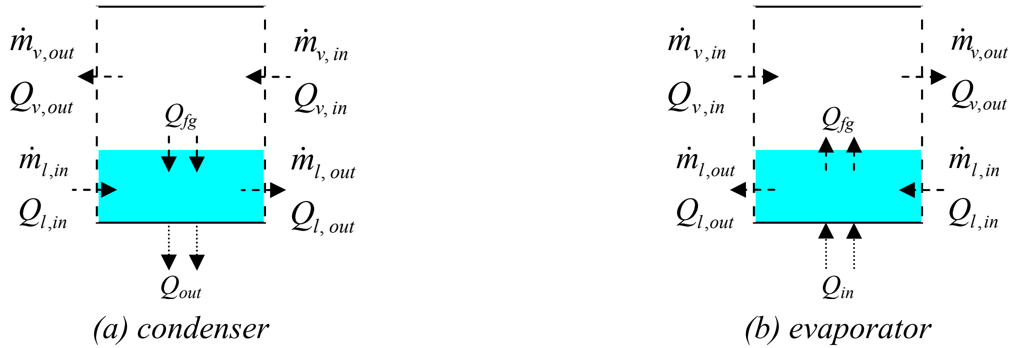

(a) condenser *(b) evaporator*

Figure 3: *Control volume in and out flows.*

Assuming that the heat capacity of the enclosure, axial conduction and other heat losses are negligible, the heat exchange with the ambient (Q_{in} and Q_{out}) has to be equal to the phase change energy. Therefore, the following energy conservation equations for condenser and evaporator regions are adopted, respectively:

$$\begin{aligned}&\frac{d}{dt}[(Ah\rho_l c_l + V_v\rho_v c_v)(T - T_r)] = -Q_{out} + A_v(\rho_{v,in}v_{v,in} - \rho_v v_{v,out})h_{fg} \\ &+ A_l[\rho_{l,in}v_{l,in}c_{l,in}(T_{l,in} - T_r) - \rho_l v_{l,out}c_l(T - T_r)] + A_v[\rho_{v,in}v_{v,in}c_{v,in}(T_{v,in} - T_r) - \rho_v v_{v,out}c_v(T - T_r)]\end{aligned} \tag{3}$$

$$\begin{aligned}&\frac{d}{dt}[(Ah\rho_l c_l + V_v\rho_v c_v)(T - T_r)] = Q_{in} - A_v(\rho_v v_{v,out} - \rho_{v,in}v_{v,in})h_{fg} \\ &+ A_l[\rho_{l,in}v_{l,in}c_{l,in}(T_{l,in} - T_r) - \rho_l v_{l,out}c_l(T - T_r)] + A_v[\rho_{v,in}v_{v,in}c_{v,in}(T_{v,in} - T_r) - \rho_v v_{v,out}c_v(T - T_r)]\end{aligned} \tag{4}$$

In these equations, a reference or system temperature is defined which is equal to the mean temperature of the outmost condenser and evaporator: $T_r = \frac{1}{2}(T_c + T_e)$. Thermodynamic properties,

such as specific heat, density and dynamic viscosity vary with temperature, and are used here with reference to this system temperature.

The energy leaving the system at the condenser (Q_{out}) is conducted through the thermal vias in the top and bottom layer of the heat pipe at the condenser region. This is modelled as a thermal resistance; therefore:

$$Q_{out} = \frac{T_c - T_{wall}}{R_{c,wall}} \tag{5}$$

where $R_{c,wall}$ represents the thermal resistance from the condenser region to the heat pipe exterior wall. Its value is derived from the thermal conductivity of the copper in the thermal vias.

Adiabatic transport sections connect the evaporator and condenser regions. The transport is governed by the momentum balance. Friction effects are estimated using hydraulic properties, as discussed by Faghri (1995), Schneider and DeVos (1980), and Shah and Bhatti (1987). The vapour momentum balance gives the following equation:

$$l_{eff} \frac{d}{dt}\left[\rho_v v_v\right] = \Delta P_v - \frac{2f\,\mathrm{Re}_{h,v}\,\mu_v l_{eff}}{D_{h,v}^2} v_v - \rho_v g l_{eff} \sin(\gamma) \tag{6}$$

As the vapour is assumed to be in a saturated state, ΔP_v can be calculated from the temperature difference. The gravitational effect is also taken into account by the last term of Equation (6). In the case of liquid transport, the momentum balance becomes:

$$l_{eff} \frac{d}{dt}\left[\rho_l v_l\right] = \Delta P_l - \frac{2f\,\mathrm{Re}_{h,l}\,\mu_l l_{eff}}{D_{h,l}^2} v_l + \rho_l g l_{eff} \sin(\gamma) \tag{7}$$

The liquid pressure difference (ΔP_l) depends on the capillary pressure produced by the wick. In theory, the wick's geometry leads to a maximum capillary pressure. This maximum is often used to determine the maximum heat transport capacity of a heat pipe. As, in this study, the liquid height in the grooves is defined by the continuity equations, a first order linearization of the maximum capillary pressure can be utilized. Hence:

$$\Delta P_l = P_{cap,\max}\left(\frac{h_{lc} - h_{le}}{h_{lc}}\right) - \Delta P_v = \frac{2\sigma}{r_{eff}}\left(\frac{h_{lc} - h_{le}}{h_{lc}}\right) - \Delta P_v \tag{8}$$

In this expression, the effective pore radius (r_{eff}) of the wick structure is equal to the width of the capillary grooves. It can be observed from Equation (8) that the pressure difference is always less than the maximum capillary pressure, as it is dependent on the liquid height in the grooves. For this reason, realistic transient simulation results can be obtained with this model.

3 Numerical simulation

A numerical prediction of the single evaporator heat pipe of Figure 1 subjected to a 15W power input is illustrated in Figure 4. The steady state mass flow rate, illustrated by the dotted line in Figure 4(a), can be calculated as:

$$\dot{m}_{ss} = \frac{Q_{in}}{h_{fg}} \tag{9}$$

where h_{fg} equals the latent heat of vaporization of water. The solid and dashed lines illustrate the time evolution of the liquid and vapour phase mass flow respectively.

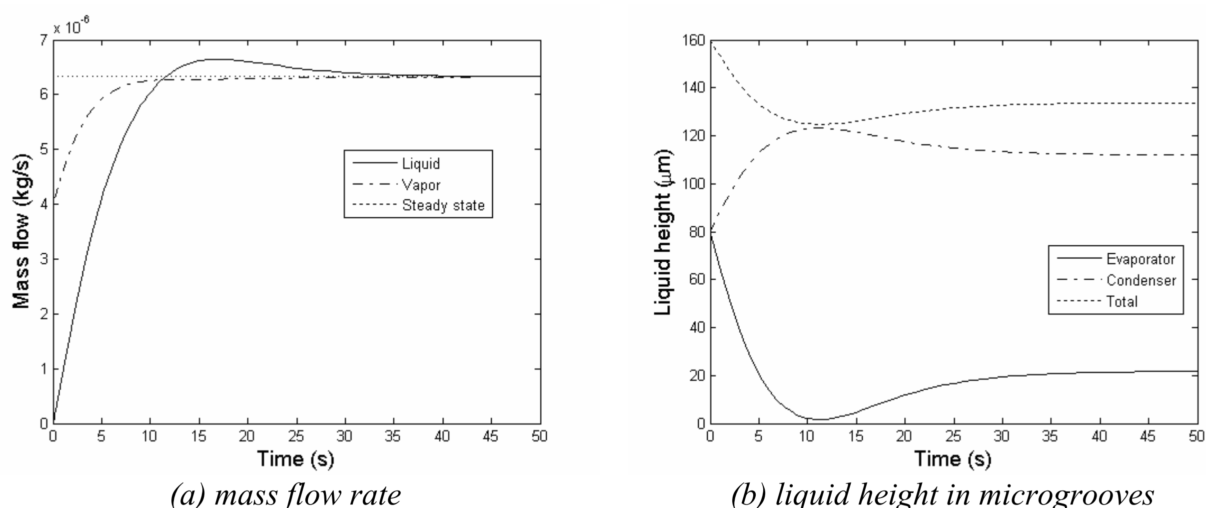

(a) mass flow rate *(b) liquid height in microgrooves*

Figure 4: *Heat pipe numerical prediction at 15W.*

Due to inertia effects, the mass flow rate of the liquid phase overshoots the steady state value by about 5%. This overshoot is a consequence of a diminishing local liquid height in the evaporator. The height of the liquid in the microgrooves is shown in Figure 4(b). Here, the solid and dashed lines indicate the liquid heights in the evaporator and condenser respectively. The dotted line indicates the sum of both. At the start of the simulation, the liquid height in the microgrooves is level: both the evaporator and the condenser heights are 80μm. As the heat pipe starts to transport heat and the system temperature increases, the total liquid height decreases. Latent energy is stored in the vapour phase, as thermodynamic properties are temperature-dependent.

Before reaching a steady state, the liquid level in the evaporator first reaches a minimum. At this point in time, a maximum in liquid pressure difference occurs (Equation 8), which accelerates the liquid flow, causing the overshoot. This minimum evaporator level at time 11s is very important for the maximum transportable power of the heat pipe. During start up, the condensate level cannot become zero, as this leads to evaporator dry-out which causes the heat pipe to stop operating. Hence, this dynamic feature of the heat pipe leads to a limit in heat transport capacity. At a later point in time, over 40s, the time derivatives have become zero in Figure 4. Here, the heat transport capacity is larger than at 15W, as the liquid level is well above zero. This is confirmed by a steady state calculation: the steady state heat transport capacity is 20W. However, this steady state capacity cannot be achieved, as the evaporator will dry out in the transient process. Hence the system dynamics limit the heat pipe performance to 15W with these parameter settings.

3.1 Two-evaporator model

The advantage of the control volume element approach, compared to e.g. finite element models, is that it can expanded with additional elements very easily. To simulate an actual PCB with multiple hot spots cooled by a flat miniature heat pipe, an additional evaporator, as shown in Figure 2(b), is added to the simulation model. The second evaporator is placed halfway the previously simulated heat pipe. As the effective length of the transported heat is a relative dominant term, a heat source located halfway can roughly dissipate double the amount of heat.

Figure 5(a) shows the operating area of such a heat pipe. Evaporator 1 (X-axis) is located at the end of the heat pipe and evaporator 2 (Y-axis) is located halfway. The dotted line shows the maximum performance of a steady state model at a system temperature of 80°C. The transient analyses are represented by the solid line. In the steady state model, evaporator 2 can approximately dissipated double the amount of heat compared to evaporator 1. Also in this case, steady state analyses result in higher predicted values than actually can be achieved when taking system dynamics into account.

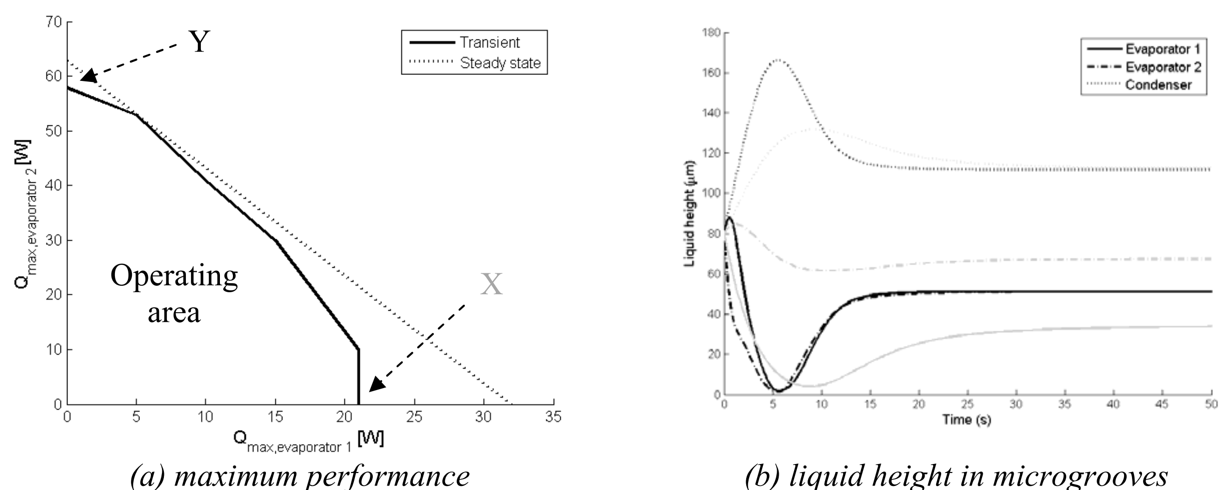

(a) maximum performance *(b) liquid height in microgrooves*

Figure 5: *Numerical prediction with two evaporators.*

Figure 5(b) shows the liquid heights in the microgrooves for the two extreme cases, X and Y, in Figure 5(a). The grey lines in figure 5(b) represent case X, i.e. all power is dissipated at the end of the heat pipe. The simulation results are similar to the single evaporator heat pipe model. Evaporator 1 almost dries out, before reaching a steady state. There is sufficient liquid at evaporator 2 at all times.

As the model contains two liquid transport sections, the first order linearization in Equation (8) expands both sections. Instead of one linear decreasing pressure term across the entire heat pipe, two are placed in series. This explains the increase in power the heat pipe is able to transport in the simulation. In practice, experimental verification should determine the amount of sections required to accurately model the heat pipe.

The black lines in Figure 5(b) represent case Y, i.e. all power is dissipated halfway the heat pipe. Both in evaporator 1 and 2 the liquid height decreases to almost zero, indicating local dry-out, before reaching a steady state. At the start of the simulation, the liquid height at evaporator 2 decreases more rapidly than at evaporator 1. Therefore, liquid flows to the middle of the heat pipe from both evaporator 1 and the condenser. When a steady state is reached, there is no difference in liquid height, and thus no flow between evaporators 1 and 2. As expected, the last section of the heat pipe does not contribute to any heat transport. Also, as the effective heat pipe length is shorter, steady state is reached faster.

4 Experimental set-up

The manufactured heat pipe, as shown in Figure 1(a) was used as a technology demonstrator for experimental verification. To drive the heat pipe, a power resistor was soldered onto the evaporator region. To monitor the heat pipe's performance, thermocouples attached to the thermal vias, and a pressure gauge were used.

The heat pipe was excited in the horizontal orientation with the previously mentioned power resistor, increasing the heat dissipation until dry-out occurred. Sufficient time was allowed to reach a steady state after each increase in power. In a second experiment, the heat pipe was oriented vertically, with gravity assisting the liquid flow. The transient response was then monitored.

5 Results and Discussion

Figure 6 illustrates the temperature distribution along the heat pipe when subjected to a thermal dissipation of 2.5 and 10W respectively. The heat pipe was able to transport the heat with a low temperature gradient along its length. For both cases, the solid and dotted lines represent the simulation predictions of the control volume model, as discussed in Section 2. The simulation reflects internal temperature values, whereas the thermocouples measure the temperature on the outside of the heat pipe. Before displaying the simulated values, it is corrected by a temperature shift dependent on the thermal resistance of the thermal vias in the condenser region ($R_{c,wall}$).

The model assumes that condensation occurs in the condenser region. In practice, this is temperature- and thus power-dependent. At 2.5W of heat dissipation, condensation occurs just over halfway along the heat pipe, as indicated by the temperature drop of the triangles in Figure 6. For the 10W case, the temperature drop and area of condensation shifts to the end of the heat pipe. At higher dissipations, the evaporator temperature rises unacceptably, indicating local dry-out.

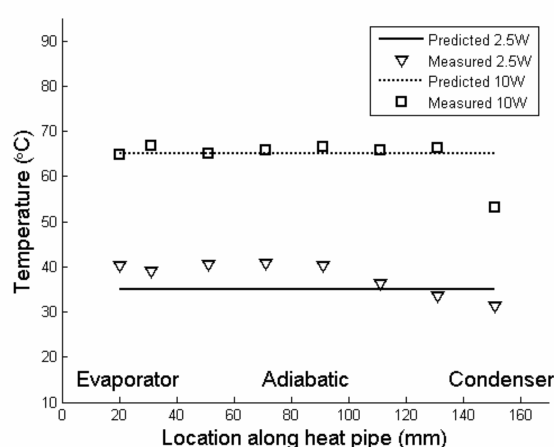

Figure 6: *Temperature distribution along the heat pipe.*

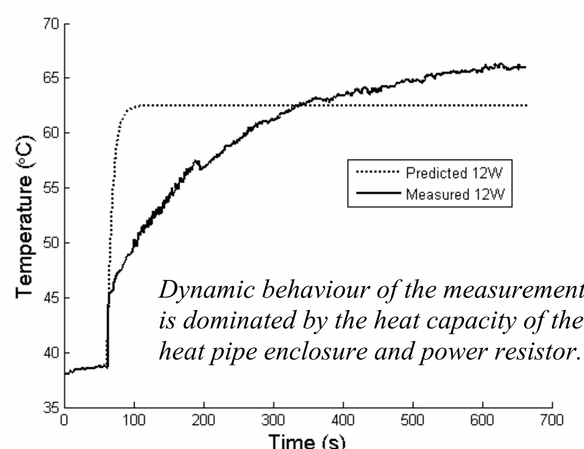

Figure 7: *Time evolution of evaporator temperature.*

Figure 7 shows the time evolution of the evaporator temperature of a vertically oriented heat pipe subject to 12W of power. The solid line indicates the measurement results, whereas the dotted line indicates the simulation prediction. The predicted steady state temperature is within a 5°C accuracy. However, the simulation model responds more quickly to a change of input than the actual heat pipe. This may be explained by the absence of heat capacitance of the enclosure in the simulation model. As no material needs to be heated up, steady state is reached more quickly. Also, the heat-up time of the power resistor is not taken into account in the simulation.

Of particular interest from a design point-of-view are the equivalent thermal conductivity and resistance coefficients from evaporator to condenser region, calculated according to Equations (9) and (10), respectively.

$$k_{eq} = \frac{Q_{in} \cdot l_{eff}}{\Delta T_{e-c} \cdot A} \quad (9)$$

$$R_{eq} = \frac{\Delta T_{e-c}}{Q_{in}} \quad (10)$$

Table 1. Equivalent thermal properties.

	Q_{in} [W]	k_{eq} [W/m·K]	R_{eq} [K/W]
Heat pipe	2.5	1006	3.8
	10	2799	1.4
Solid copper	-	400	9.7

The thermal properties of both measurements, as well as those of solid copper, are listed in Table 1. In the case of 10W dissipation, the equivalent thermal conductivity of the heat pipe reaches approximately seven times the conductivity of solid copper. This is a good illustration of the high efficiency of the heat pipe for cooling purposes.

Theoretically, every Watt dissipated by an electronic component, soldered onto the PCB, may cause as little as 1.4K temperature increase from the component to the condenser area in a horizontal set-up. In practice this rule is limited, as the heat pipe may eventually dry out in the evaporator area. It must also be noted that in this approximation, heat transfer from the condenser to the environment is assumed to be unrestricted.

Compared to the theoretical figures presented in Section 3, the heat pipe transports less power than calculated. This discrepancy may be explained by the hypothesis of an optimal wetted wick structure. In practice, this assumption may be adversely influenced by small amounts of contamination on the board layers or in the water. Also, the temperature drop at the condenser region in Figure 6 may indicate the presence of non-condensable gases.

6 Conclusions

A heat pipe constructed in a PCB is a very effective means of heat transport, for the investigated parameter settings about seven times more effective than solid copper. The model indicates that the steady state performance is limited by the system dynamics. The maximum heat transport capacity is limited by the minimum height of the liquid level in the evaporator during start up. This dynamic feature is caused by the inertia and storage of carrier fluid in the system. The model performance is validated by an experiment. Model predictions for maximum power and system temperatures compare well with measurements. However, the time scale for start up is under estimated, probably due to the negligence of thermal capacity of the enclosure. The effect of this thermal inertia is expected not to have an influence on the qualitative aspects of the system. Nevertheless, in future work the model will be extended to take the enclosure's heat capacity into account and thus validate system dynamics. Also, the two-evaporator heat pipe model will be validated experimentally.

Acknowledgments

This work is part of the PACMAN project which is supported by the Netherlands Ministry of Economic Affairs, SenterNovem project number TSIT3049. The authors especially want to thank Hans Adelaar, Bennie van Bloem, Mark de Gier, Rob Legtenberg and Jan Mannak for their assistance with heat pipe development and experiments. The authors also thank the PCB production and electronics assembly department of Thales Nederland for their assistance during the production of the prototypes.

References

Cao, Y., Faghri, A. and Mahefkey, T., 1993, Micro/Miniature Heat Pipes and Operating Limitations, ASME HTD-Vol. 236, pp. 55-62

Faghri, A., 1995, Heat Pipe Science and Technology, Taylor & Francis, New York, USA.

Schneider, G.E. and DeVos, R., 1980, Nondimensional Analysis for the Heat Transport Capability of Axially-Grooved Heat Pipes Including Liquid/Vapor Interaction, AIAA Paper No. 80-0214.

Shah, R.K. and Bhatti, M.S., 1987, Laminar Convective Heat Transfer in Ducts, Handbook of Single-Phase Convective Heat Transfer, New York.

Vincent, C.C.J. and Kok, J.B.W., 1992, Investigation of the overall transient performance of the industrial two-phase closed loop thermosyphon, International Journal of Heat and Mass Transfer, Vol. 35, No. 6, pp. 1419-1426.

Wits, W.W., Legtenberg, R., Mannak, J. and Zalk, B. van, 2006, Thermal Management through In-Board Heat Pipes Manufactured using Printed Circuit Board Multilayer Technology, Proc. International Electronic Manufacturing Technology (IEMT), Putrajaya, Malaysia, pp. 55-61.

View publication stats